Bollettino
Unione Matematica Italiana

Paolo Biscari, Stefano Turzi

Asymptotic Director Fields of Moving Defects in Nematic Liquid Crystals

Bollettino dell'Unione Matematica Italiana, Serie 9, Vol. **5** (2012), n.1, p. 81–91.

Unione Matematica Italiana

<http://www.bdim.eu/item?id=BUMI_2012_9_5_1_81_0>

Bollettino dell'Unione Matematica Italiana, Unione Matematica Italiana, 2012.

Bollettino U. M. I.
(9) **V** (2012), 81-91

Asymptotic Director Fields of Moving Defects in Nematic Liquid Crystals

PAOLO BISCARI - STEFANO TURZI

Abstract. – *This paper deals with the detailed structure of the order-parameter field both close and far from a moving singularity in nematic liquid crystals. We put forward asymptotic expansions that allow to extract from the exact solution the necessary analytical details, at any prescribed order. We also present a simple uniform approximation, which captures the qualitative features of the exact solution in all the domain.*

This paper is dedicated to the memory of Carlo Cercignani, a master who will be never praised enough for both his scientific achievements and the way he taught how research is to be conducted.

Nematic liquid crystals are aggregates of (quasi) axially-symmetric molecules which aim at orienting along a common, parallel direction. Boundary conditions and/or external fields may, however, induce non trivial configurations and, under some special circumstances, singularities in the orientation field. These *defects* have been extensively studied over the last decades and have played a propelling role in the establishment of the *Topological theory of defects* [1, 2, 3]. By studying the homotopy groups of the order parameter manifold, it becomes possible to assign a topological charge to each singularity. The total topological charge is invariant under regular evolution of the system, but single defects may split and/or annihilate [4, 5], while pairs of opposite-charged defects may emerge in otherwise regular patterns [6].

In recent years, attention has been focused on the possibility of driving the defect dynamics through suitable external fields [7, 8]. Analytical relations between the defect velocity and the external field intensity and direction have been established in [9] by neglecting *backflow*, *i.e.* the orientational modifications induced by the presence of a macroscopic flow, and vice versa. Neglecting backflow is a non-trivial simplification. Indeed, both numerical [10] and experimental [11] studies have stressed the importance of backflow effects, including the speed difference between opposite-charged defects. Nevertheless, it has been recently shown [12] that the no-backflow solution can be interpreted as the leading-order term in a perturbation scheme. In such an iterative procedure, both the macroscopic velocity field and the corrections to the defect speed may

be computed in terms of the no-backflow solution. In particular, the symmetries of the no-backflow solution determine which Fourier components of the velocity field influence the general solution. It becomes therefore important for applications to understand in detail the structure of the orientation field obtained in the absence of backflow.

In this paper we analyze the no-backflow solution identified in [9]. By suitably adapting classical perturbation methods, we extract analytical information about the qualitative features of the orientational pattern of a moving defect in all the relevant domains: close to the defect, in the characteristic π-wall, and far from the defect. In all cases, we test the analytical approximations against the outcomes of numerical simulations. Close to the defect, we show that the defect speed does not break the symmetry of the stationary pattern at the leading order. Far from the singularity, we are able to prove the existence, and to determine the structure of a translationally invariant wall. We also identify a quite simple, uniform approximation, that approximates remarkably well the exact solution in all the regions.

The plan of the paper is as follows. In the next section, we review the relevant equations of the nematic defects evolution, and set up the geometry of the model under study. Sections 2 and 3 are devoted to the asymptotic expansions of the orientational pattern. Finally, in Section 4 we introduce the uniform approximation, and test the analytical predictions against the results of numerical computations.

1. – Stationary motion of a nematic defect

The order parameter fit to describe the microscopic configuration of a nematic liquid crystal is the *director* field $\boldsymbol{n} : \mathcal{B} \to S^2$, where $\mathcal{B}$ is the region occupied by the system under study, S^2 is the unit sphere in $\mathbb{R}^3$, and therefore $\boldsymbol{n}(P)$ is a unit vector pointing parallel to the molecular orientation at the point $P \in \mathcal{B}$. In addition, the head-and-tail symmetry of nematic molecules implies that the orientations $\boldsymbol{n}$ and $-\boldsymbol{n}$ must be considered as equivalent. Therefore, the order parameter manifold will be actually identified with the quotient set $S^2/\sim$, which coincides with the projective plane $\mathbb{RP}^2$. Nematic defects are the discontinuities of the map $\boldsymbol{n}$. In this paper we deal with *nematic disclinations*, that is line singularities. More precisely, we take $\mathcal{B}$ to be coincident with $\mathbb{R}^3$, and assume translational invariance along the z-direction, so that we may restrict our attention to the plane $\mathcal{B}_0 = \{z = 0\}$. The disclination is represented by a line orthogonal to $\mathcal{B}_0$ and, in our treatment, its position will therefore be identified by a point in $\mathcal{B}_0$.

Nematic disclinations may be classified on the basis of the number of turns η the director performs when we follow its variation along a closed curve which includes the defect. The head-and-tail symmetry described above implies that the topolo-

gical charge η may take half-integer values. We consider a $\eta = \pm\frac{1}{2}$ disclination moving in an external magnetic field, as described in detail in [9]. The external field is assumed to favor the director orientation of one side of the defect with respect to the other side, and this asymmetry is sufficient to induce a defect motion. We follow the so-called *one-constant approximation* in the choice of the hyperelastic potential which determines the energetic cost of any prescribed configuration $\boldsymbol{n}$, and neglect backflow. More precisely, we are interested in determining the shape and the speed of a steadily-moving pattern in which the defect proceeds towards its preferred direction. To this aim, we choose a co-moving reference frame, in which the direction configuration appears as still, with the direction sitting at the origin O. The x-axis is chosen to be parallel to the external field. Given any point P in the plane, let (r, θ) be the polar coordinates of P in $\mathcal{B}_0$, and let $\phi(P)$ be the angle the nematic director at P determines with the x-axis (see Figure 1).

We refer to [9] for the analytical details in determining the travelling pattern which describes an η-disclination (with $\eta = \pm\frac{1}{2}$) and satisfies $\phi(P) = 0$ in the positive x-axis. Such solution is given by

$$\phi(x,y) = \begin{cases} \eta\,\dfrac{\pi}{2}\,\mathrm{e}^{-\frac{y}{\xi}} - \eta \displaystyle\int_0^{+\infty} \mathrm{Im}\left(\mathrm{e}^{iqx-k_q y}\right)\frac{dq}{q} & \text{if } y \geq 0\,, \\ -\phi(x,-y) & \text{otherwise.} \end{cases} \tag{1}$$

In (1), $\xi = \sqrt{K/(\chi_{\mathrm{a}} H^2)}$ represents the magnetic coherence length, with K the average Frank nematic elastic constant, χ_{a} the magnetic anisotropy, and H the intensity of the external field. Moreover, k_q is defined as the square root of the equation $k_q^2 = q^2 + iq\gamma + \xi^{-2}$ which has positive real part. Finally, $\gamma = \gamma_1 v/(2K)$ is a parameter (proportional to the defect speed v and the nematic viscosity γ_1), which has the dimensions of an inverse length. The defect speed v can be determined through the self-consistency equation

$$\int_0^{\xi/r_0} \left(\sqrt{1 + \frac{\mathrm{i}\gamma\xi}{s} + \frac{1}{s^2}} - \sqrt{1 - \frac{\mathrm{i}\gamma\xi}{s} + \frac{1}{s^2}}\right) ds = \mathrm{i}\pi, \tag{2}$$

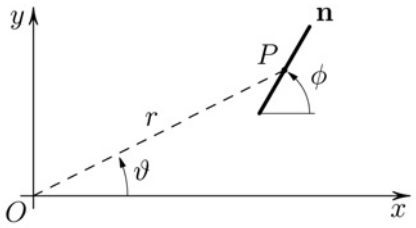

Fig. 1. - Coordinates definition in the problem under study.

where r_0 is a microscopic length, of the size of the defect core within which the nematic undergoes a phase transition towards an isotropic, or a biaxial phase [13]. It is typically well below the μm scale and then much smaller than all other characteristic lengths. Figure 3 in [9] shows how the solutions of equation (2) precisely depend on the ratio ξ/r_0. For our purposes, we may simply recall that, for values covering most applications, the speed v turns out to be proportional to the magnetic coherence length, apart from a logarithmic correction.

The next sections will be devoted to a careful asymptotic analysis of the director field (1). Because of the top-down symmetry evidenced in it, we will restrict our attention to the upper half-plane in $\mathcal{B}_0$. First of all, it is convenient to transform the integrand in (1). By solving the algebraic equation which defines k_q and then choosing the correct solution, it is possible to show that, for any $y > 0$,

$$\phi(x,y) = \eta\frac{\pi}{2}\mathrm{e}^{-\bar{y}} - \eta\int_0^{+\infty} \mathrm{e}^{-\bar{y}/g_\lambda(\bar{q})}\sin\bar{q}\left(\bar{x} - \lambda\bar{y}g_\lambda(\bar{q})\right)\frac{d\bar{q}}{\bar{q}} \tag{3}$$

where all variables identified with a bar are now dimensionless: $\bar{x} = x/\xi$, $\bar{y} = y/\xi$, $\bar{q} = q\xi$. Moreover, $\lambda = \frac{1}{2}\gamma\xi$, is a speed-dependent dimensionless parameter, of order 1. Finally, the function g_λ is defined as

$$g_\lambda(t) = \frac{\left(\sqrt{(1+t^2)^2 + 4\lambda^2t^2} - 1 - t^2\right)^{\frac{1}{2}}}{\sqrt{2}\lambda t} \quad \text{for } t > 0, \tag{4}$$

with $g_\lambda(0) = 1$. A straightforward analysis of its first derivative suffices to show

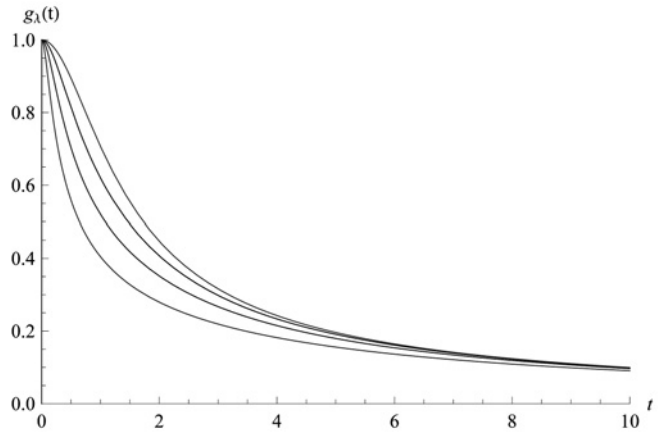

Fig. 2. - Plot of the function g_λ defined in (4) for different values of λ. Top to bottom: limit $\lambda \to 0^+$, $\lambda = \frac{5}{2}, 5, 10$.

that g_λ is a monotonically decreasing function of t for any positive t and that

$$0 = \lim_{t\to+\infty} g_\lambda(t) \leq g_\lambda(t) \leq \lim_{t\to 0^+} g_\lambda(t) = 1 \quad \forall t > 0,\ \forall \lambda > 0.$$

More precisely,

$$g_\lambda(t) = 1 - \frac{1}{2}(1+\lambda^2)t^2 + O(t^4) \text{ when } \quad t \to 0^+,$$

(5)

$$g_\lambda(t) = \frac{1}{t} - \frac{1}{2}(1+\lambda^2)\frac{1}{t^3} + O\left(\frac{1}{t^5}\right) \text{ when } \quad t \to +\infty.$$

Figure 2 evidences that g_λ does not depend critically on the particular value attained by the parameter λ, as long as it remains within the range of physical interest.

2. – Far-from-defect approximation

To begin with, we determine the asymptotic shape of the director configuration at points P sufficiently far from the defect, which sits at the origin of the co-moving reference frame.

2.1 – *Far field*

We begin by considering the easiest case, *i.e.* the limit $\bar{y} \gg 1$ ($y \gg \xi$). In this case we may apply the Laplace method [14] for the asymptotic expansion of the integral in (3) when $\bar{y} \to +\infty$. The main contribution to the integral, in the limit $\bar{y} \to +\infty$, arises from the values of $\bar{q}$ such that $-1/g_\lambda(\bar{q})$ attains its maximum. In view of the remarks above on the function g_λ, this certainly occurs as $q \to 0^+$. Therefore, it is only the immediate neighborhood of $q = 0$ that contributes to the full asymptotic expansion of the integral for large $\bar{y}$, and we may replace g_λ with its Taylor expansion about $q = 0$. The resulting approximation of equation (3) is

$$\phi(x,y) \sim \eta\, \mathrm{e}^{-\bar{y}} \left(\frac{\pi}{2} - \int_0^{+\infty} \mathrm{e}^{-\frac{1}{2}\bar{q}^2\bar{y}\left(1+\lambda^2\right)} \sin\bar{q}(\bar{x} - \lambda\,\bar{y})\, \frac{d\bar{q}}{\bar{q}} \right).$$

This integral can be explicitly computed in terms of the error function

$$\mathrm{erf}(z) = \frac{2}{\sqrt{\pi}} \int_0^z \mathrm{e}^{-t^2} dt.$$

We obtain

$$\phi(x,y) \sim \eta \,\frac{\pi}{2}\, \mathrm{e}^{-\bar{y}} \left(1 - \operatorname{erf} \frac{\bar{x} - \lambda \bar{y}}{\sqrt{2(1+\lambda^2)\bar{y}}} \right) \quad \text{as } \bar{y} \gg 1. \tag{6}$$

In particular, and since $|\operatorname{erf}(z)| < 1$ for any $z \in \mathbb{R}$, the tilt angle ϕ decays exponentially with $\bar{y}$ when this latter increases.

2.2 – *π-wall*

The approximation (6) has in fact a wider range of validity than expected. Indeed, the same conclusion about the integral (3) being dominated by the small-$\bar{q}$ terms can be applied also when the factor multiplying $\bar{q}$ in the argument of the sine function becomes large. Such a factor can be given the following bounds, uniform in $\bar{q}$:

$$\big| |\bar{x}| - |\lambda \bar{y}| \big| \leq \big| \bar{x} - \lambda \bar{y} g_\lambda(\bar{q}) \big| \leq |\bar{x}| + \lambda \bar{y}, \quad \forall \bar{x} \in \mathbb{R},\ \forall \bar{y}, \bar{q}, \lambda \geq 0. \tag{7}$$

Therefore, the approximate expression (6) becomes valid also if $|\bar{x}|$ is large, while $\bar{y}$ remains finite. In particular, it is interesting to check the behavior of the solution close to the x axis, in order to appreciate the difference between the left and the right-hand sides of the defect. Since

$$\operatorname{erf}(t) = \quad 1 - \frac{\mathrm{e}^{-t^2}}{\sqrt{\pi}\, t} \left(1 - \frac{1}{2t^2} + O\big(t^{-4}\big) \right) \qquad \text{as } t \to +\infty$$

$$\operatorname{erf}(t) = -1 - \frac{\mathrm{e}^{-t^2}}{\sqrt{\pi}\, t} \left(1 - \frac{1}{2t^2} + O\big(t^{-4}\big) \right) \qquad \text{as } t \to -\infty,$$

we obtain at leading order

$$\phi(x,y) \sim \eta \sqrt{\frac{\pi(1+\lambda^2)\bar{y}}{2\bar{x}^2}}\, \mathrm{e}^{-\bar{y} - \frac{\bar{x}^2}{2(1+\lambda^2)\bar{y}}} \qquad \text{as } \bar{x} \to +\infty \quad (\bar{y} > 0 \text{ fixed}) \tag{8}$$

$$\phi(x,y) \sim \eta\, \pi\, \mathrm{e}^{-\bar{y}} \qquad \text{as } \bar{x} \to -\infty \quad (\bar{y} > 0 \text{ fixed}). \tag{9}$$

The estimate (8) shows that at the right-hand side of the defect the tilt angle decays exponentially towards the direction preferred by the external field. On the contrary, equation (9) shows that at the left-hand side of the defect there is a structure which does not vanish at infinity. Whatever the (large and negative) value of $\bar{x}$, the director performs a rotation of $\eta\pi$ in a vertical strip of characteristic length ξ. More precisely, and in view of the top-down symmetry of the

field about the x-axis, the director performs a $2\eta\pi$ rotation in a strip of typical size 2ξ. Since we restrict the attention to $\eta = \pm\,\frac{1}{2}$ (which is indeed the only energetically stable choice) such a stripe is thus identified as a *π-wall*. Both the elastic and the magnetic energies induced by the defect are mostly confined in this domain, as evidenced in Figure 2 of [9].

3. – Close-to-defect approximation

At equilibrium, and within the one-constant approximation, all planar nematic point singularities tend to a universal asymptotic pattern when we approach the defect [15]:

$$\phi(r,\theta) \sim \eta\theta + \text{const.}, \quad \text{as } r \to 0. \tag{10}$$

It is our present aim to check whether such approximation stands in the case of a stationarily-moving defect, and possibly to compute the first-order corrections to the asymptotic limit. We stress that it is not trivial *a priori* that the limiting pattern obeys equation (10), because the presence of the external field and the π-wall clearly breaks the rotational symmetry around the defect.

Close to the defect, the gradients of the director field diverge. This implies that the Fourier integral in (3) is expected to be dominated by the large-$\bar{q}$ contributions. Similar conclusions may be drawn by noticing that the estimate (7) evidences that the factor multiplying $\bar{q}$ in the argument of the sine function vanishes close to the defect.

Once we take into account the asymptotic expansion (5) for g_λ, the integral in equation (3) simplifies to the Laplace transform

$$\operatorname{Im}\left\{ \mathrm{e}^{-i\lambda\bar{y}} \int_0^{+\infty} \mathrm{e}^{-s\bar{q}} \exp\left(-\frac{1+\lambda^2}{2}\frac{\bar{y}}{\bar{q}} \right) \frac{d\bar{q}}{\bar{q}} \right\},$$

where the Laplace variable s, is to be evaluated in $s = \bar{y} - i\bar{x}$. The interesting feature of this approximation is that it is possible to compute analytically the Laplace transform of $\exp(-C/\bar{q})/\bar{q}$, where C is a positive constant (see *e.g.* [16]). Therefore, we obtain the following approximation of the director field close to the defect

$$\phi(x,y) \sim \eta\frac{\pi}{2}\mathrm{e}^{-\bar{y}} - \eta \operatorname{Im}\left\{ 2\,\mathrm{e}^{-i\lambda\bar{y}} K_0\left(\sqrt{2(1+\lambda^2)(\bar{y}^2 - i\bar{x}\bar{y})} \right) \right\}, \tag{11}$$

where $K_0(z)$ is the zeroth-order modified Bessel function of the second kind.

In the limit $\bar{x}, \bar{y} \ll 1$, the modified Bessel function can be approximated by its leading order terms $K_0(z) \sim -\log(z/2) - \Gamma$, where Γ is Euler's constant, with

numerical value $\Gamma \doteq 0.577216$. After some further algebra, equation (11) becomes

$$\phi(r,\theta) = \eta\theta - \frac{\eta r \sin\theta}{2\xi}\left[\pi + 4\lambda\Gamma + \lambda \log \frac{r^4(1+\lambda^2)^2 \sin^2\theta}{4\xi^4}\right] + O(r^2), \tag{12}$$

as $r \to 0$.

Equation (12) shows that the stationary pattern of a moving defect shares the same asymptotic behavior (10) of a stationary singularity. The rotational symmetry is broken at $O(r)$, the maximum asymmetry being concentrated above and below the defect.

4. – A uniform approximation and numerical tests

The structure of the far- and close-to-defect approximations (in particular equations (9) and (12)) suggests to propose a simple, uniform approximation, which turns out to be able to match asymptotically both limits. Such approximation is given by

$$\phi(r,\theta) = \eta\theta\, \mathrm{e}^{-r\sin\theta/\xi}, \tag{13}$$

and it is immediate to check that it satisfies all the boundary requirements. It is the aim of the present section to test all the asymptotic and uniform approximations derived above against the results of exact calculations, performed through suitable numerical integration routines.

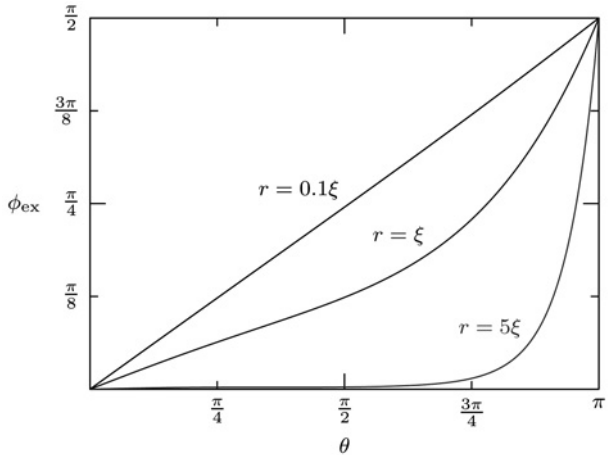

Fig. 3. - A plot of the the exact solution $\phi_{\mathrm{ex}}(r,\theta)$, as given in (1), computed along half-circles of radii (top to bottom) $r = 0.1\xi$, $r = \xi$, and $r = 5\xi$. The parameter λ is set to 0.5, and $\eta = +\frac{1}{2}$.

We report the results obtained by comparing the predictions along three half-circles, all centered in the defect and of radii $r = 0.1\xi$, $r = \xi$ and $r = 5\xi$ respectively. The dimensionless parameter λ is set to be equal to 0.5, a value which matches the predictions computed in [9], and reported in Figure 3 therein. The sign of the topological charge of the defect does not affect critically the results, as η everywhere appears simply as a multiplying factor. In the following we set $\eta = +\frac{1}{2}$.

Figure 3 reports the results of the exact calculations. To make explicit comparisons, in Figures 4 and 5 we have plotted the errors of the approximated analytical solutions, defined as the difference $\Delta\phi = \phi_{\text{asy}} - \phi_{\text{ex}}$.

Close to the defect (see Figure 4(a)), the dashed line corresponding to the approximate solution (12) obviously provides the best results. It is however to be remarked that the dotted line, corresponding to the uniform approximation (13), provides only slightly greater errors. At intermediate distances (see Figure 4(b)), the close-to-defect approximation immediately looses validity, as it does not capture the decay of the director towards the direction established by the external field. The uniform and far-field approximations are approximately equivalent in this range. When we finally reach the far-from-defect domain (see Figure 5) the close-to-defect approximation is meaningless, and there is no sense in reporting it. On the contrary, the uniform approximation (13) is not to be discarded, as the error scale in this Figure has been augmented for the ease of presentation.

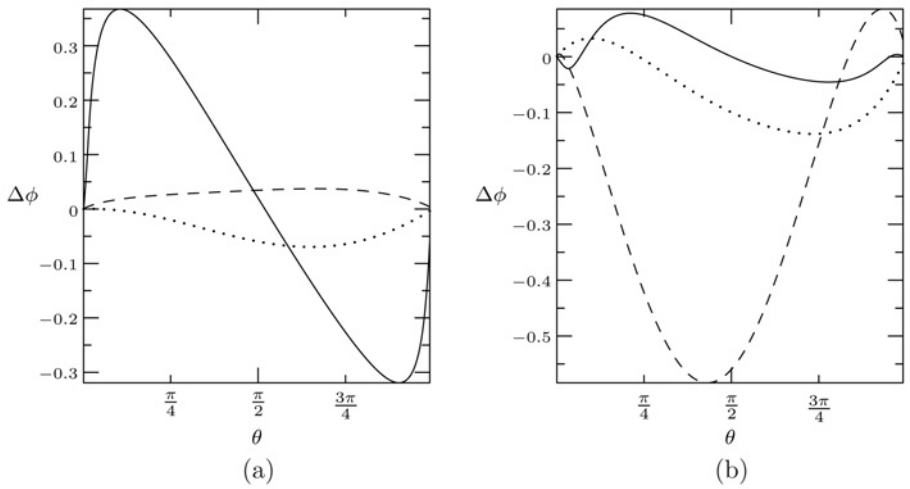

Fig. 4. - Comparison of the errors $\Delta\phi = \phi_{\text{asy}} - \phi_{\text{ex}}$ between the exact solution, as given in (1), and the three approximate solutions (6) (solid line), (12) (dashed line) and (13) (dotted line). The errors are calculated along a half-circle of radius (a) $r = 0.1\xi$ and (b) $r = \xi$. The value of the parameter λ is set to 0.5, and $\eta = +\frac{1}{2}$.

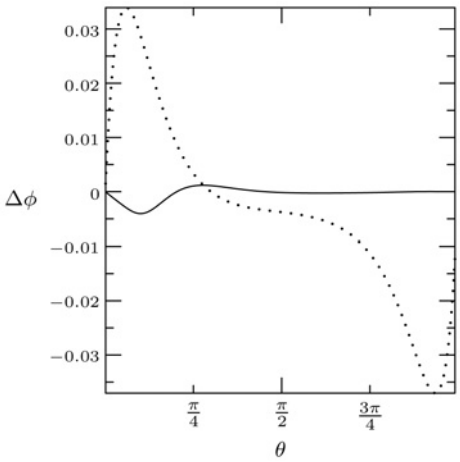

Fig. 5. - Same as in Figure 4 except that $r = 5\xi$. For this value of r, the close-to-defect approximation yields too large errors, and it is therefore not shown here. Note the change of scale in the error axis with respect to Figure 4.

To summarize: we have established classical perturbation expansions that allow us to obtain asymptotic analytical expressions for the director field of a moving nematic defect. Moreover, we have presented in this section a new, uniform approximation, that proves useful to capture the qualitative features of the director field both close and far from the defect.

Acknowledgement. We want to thank the unknown Referee for his/her very useful suggestions on the manuscript.

REFERENCES

[1] N. D. MERMIN, *The topological theory of defects in ordered media*, Rev. Mod. Phys., **51** (1979), 591-648.
[2] M. KLÉMAN, *Defects in liquid crystals*, Rep. Prog. Phys., **52** (1989), 555-654.
[3] P. BISCARI - G. GUIDONE-PEROLI, *A hierarchy of defects in biaxial nematics*, Commun. Math. Phys., **186** (1997), 381-392.
[4] G. GUIDONE-PEROLI - E. G. VIRGA, *Annihilation of point defects in nematic liquid crystals*, Phys. Rev. E, **54** (1996), 5235-5241.
[5] P. BISCARI - G. GUIDONE-PEROLI - E. G. VIRGA, *A statistical study for evolving arrays of nematic point defects*, Liquid Crystals, **26** (1999), 1825-1832.
[6] G. GUIDONE-PEROLI - E. G. VIRGA, *Nucleation of topological dipoles in nematic liquid crystals*, Commun. Math. Phys., **200** (1999), 195-210.
[7] G. RYSKIN - M. KREMENETSKY, *Drag force on a line defect moving through an otherwise undisturbed field: Disclination line in a nematic liquid crystal*, Phys. Rev. Lett., **67** (1991), 1574-1577.

[8] E. I. Kats - V. V. Lebedev - S. V. Malinin, *Disclination motion in liquid crystalline films*, J. Exp. Theor. Phys., **95** (2002), 714-727.
[9] P. Biscari - T. J. Sluckin, *Field-induced motion of nematic disclinations* SIAM J. Appl. Math., **65** (2005), 2141-2157.
[10] D. Svenšek - S. Žumer, *Hydrodynamics of pair-annihilating disclination lines in nematic liquid crystals*, Phys. Rev. E, **66** (2002), 021712.
[11] C. Blanc - D. Svenšek - S. Žumer - M. Nobili, *Dynamics of nematic liquid crystal disclinations: The role of the backflow*, Phys. Rev. Lett., **95** (2005), 097802.
[12] P. Biscari - T. J. Sluckin, *A perturbative approach to the backflow dynamics of nematic defects*, Euro. J. Appl. Math. **23** (2012), 181-200.
[13] P. Biscari - G. Guidone-Peroli - T. J. Sluckin, *The topological microstructure of defects in nematic liquid crystals*, Mol. Cryst. Liq. Cryst., **292** (1997), 91-101.
[14] C. Bender - S. Orszag, *Advanced Mathematical Methods for Scientists and Engineers*, Springer-Verlag, New York (1999).
[15] H. Brezis - J. M. Coron - E. Lieb, *Harmonic maps with defects*, Comm. Math. Phys., **107** (1986), 649-705.
[16] M. Abramowitz - I. Stegun, *Handbook of Mathematical Functions with Formulas, Graphs, and Mathematical Tables*, Dover Publications (1965).

Paolo Biscari: Dipartimento di Matematica, Politecnico di Milano
Piazza Leonardo da Vinci 32, 20133 Milan, Italy
E-mail: paolo.biscari@polimi.it

Stefano Turzi: Università degli Studi e-Campus
Via Isimbardi 10, 22060 Novedrate (CO), Italy.
E-mail: stefano.turzi@polimi.it

Received May 11, 2011 and in revised form June 16, 2011